

# Ammonia is a hydrogen carrier in the regeneration of Pt/BaO/Al<sub>2</sub>O<sub>3</sub> NO<sub>x</sub> traps with H<sub>2</sub>

L. Cumararatunge<sup>a</sup>, S.S. Mulla<sup>a</sup>, A. Yezerets<sup>b</sup>, N.W. Currier<sup>b</sup>, W.N. Delgass<sup>a</sup>, F.H. Ribeiro<sup>a,\*</sup>

<sup>a</sup> School of Chemical Engineering, Purdue University, Forney Hall of Chemical Engineering, 480 Stadium Mall Drive, West Lafayette, IN 47907-2100, USA

<sup>b</sup> Cummins Inc., 1900 McKinley Ave, Columbus, IN 47201, USA

Received 15 September 2006; revised 7 November 2006; accepted 7 November 2006

Available online 14 December 2006

## Abstract

We report that the regeneration of a Pt/BaO/Al<sub>2</sub>O<sub>3</sub> NO<sub>x</sub> trap in H<sub>2</sub> occurs through the formation of NH<sub>3</sub> as an intermediate. When NH<sub>3</sub> is used instead of H<sub>2</sub>, the reduction process is equivalent and equally effective to using H<sub>2</sub>, thus confirming our hypothesis. The regeneration is localized, occurring at the plug flow front and is limited by mass transfer of the gas phase reductant to the catalyst. The process is consistent with the release of NO<sub>x</sub> from the trapping material, followed by its reduction over Pt. The high selectivity of Pt/BaO/Al<sub>2</sub>O<sub>3</sub> in forming mostly N<sub>2</sub> during regeneration is achieved by the release of NO<sub>x</sub> only in the presence of H<sub>2</sub> which guarantees the formation of N<sub>2</sub> and NH<sub>3</sub> and only small amounts of N<sub>2</sub>O. An oxygen source on the catalyst support, usually the stored NO<sub>x</sub>, is necessary for the oxidation of NH<sub>3</sub> to N<sub>2</sub>.

© 2006 Elsevier Inc. All rights reserved.

**Keywords:** Mechanism of reduction of NO<sub>x</sub> traps; Pt/BaO/Al<sub>2</sub>O<sub>3</sub> NO<sub>x</sub> traps; Ammonia as a NO<sub>x</sub> reduction intermediate

## 1. Introduction

The NO<sub>x</sub> storage/reduction (NSR) process is one of the technologies in development to abate the NO<sub>x</sub> (NO + NO<sub>2</sub>) in the exhaust emitted from combustion engines. This system works by the Pt catalyst transforming the NO in the exhaust to NO<sub>2</sub>, which then reacts with a barium or potassium component to form a stable compound, which is periodically reduced to release most of the nitrogen as N<sub>2</sub> [1]. This cycle of oxidation, trapping, release and reduction is performed, for example, with a 60 s capture (oxidation and trapping) followed by a four second regeneration (release and reduction). On a commercial system, the efficiency in transforming the emitted NO<sub>x</sub> to N<sub>2</sub> is over 95%. This is remarkable, as the Pt itself is selective for the formation of N<sub>2</sub> from NO and H<sub>2</sub> only in a narrow range of NO to H<sub>2</sub> ratio, as reported in the literature [2,3] and as we will show below. A more detailed account of this technology can be found in a recent review [4].

A few studies have been devoted to the analysis of the regeneration or the reduction phase. Burch and Millington [5] proposed a mechanism in which NO is decomposed on reduced Pt sites, and the role of the reductant is to reduce the oxidized Pt to Pt<sup>0</sup>, which is capable of reducing NO to N<sub>2</sub>. On the other hand, direct reaction between released NO<sub>x</sub> species and the reductant molecules on the precious metal has also been proposed [6]. Here the debate on the possible mechanism governing NO<sub>x</sub> release remains open. Kabin et al. [7] proposed that the NO<sub>x</sub> is released as a result of the heat generated by the exothermic reactions upon switching to the regenerating gases (thermal release), while others have proposed a decrease in the equilibrium stability of the stored nitrates due to either the decrease in the partial pressure of oxygen [8,9] or the establishment of a net reducing environment [9,10]. In addition, Liu and Anderson [9] have proposed a different mechanism of NO<sub>x</sub> release in which the reductant molecule (or its activated form spilled over from Pt) may interact directly with the stored NO<sub>x</sub> on the storage component where the nitrates are reduced to nitrites which then release NO and gaseous oxygen. Recently, Nova et al. [11] reported a similar mechanism that involves the activation of H<sub>2</sub> on Pt sites, followed by spillover on the alumina support toward

\* Corresponding author. Fax: +1 765 494 0805.

E-mail address: [fabio@purdue.edu](mailto:fabio@purdue.edu) (F.H. Ribeiro).

nitrate adspecies that decompose to gaseous NO<sub>x</sub>, which is then reduced on Pt or is directly reduced by spilled over hydrogen. They also included the possibility of a mechanism involving surface diffusion of NO<sub>x</sub> adspecies toward reduced Pt sites, which reduce the NO<sub>x</sub> to N<sub>2</sub>.

The objective of this contribution is to gain further insight into the mechanism governing the reduction of stored NO<sub>x</sub> species and provide a model of how the reduction process occurs, including why it is so selective to N<sub>2</sub>. We will show that the reduction process can be explained by the release of NO or NO<sub>2</sub> which is then optimally reduced to N<sub>2</sub> or over-reduced to NH<sub>3</sub> on the Pt clusters. If N<sub>2</sub>O is formed, most of it continues to react with hydrogen on the Pt surface to form N<sub>2</sub> or NH<sub>3</sub>. Most importantly, we will show that the NH<sub>3</sub> formed is as effective as H<sub>2</sub> in the reduction/regeneration process and is eventually transformed to N<sub>2</sub>.

## 2. Experimental methods

The Pt/Al<sub>2</sub>O<sub>3</sub> and Pt/BaO/Al<sub>2</sub>O<sub>3</sub> catalysts used in this study were supplied by EmeraChem in monolithic form. Both monoliths had a cell density of 200 channels per in<sup>2</sup>. The Pt loading for both samples was ca. 50 g ft<sup>-3</sup> of monolith. The Ba loading in the Pt/BaO/Al<sub>2</sub>O<sub>3</sub> sample was 20 wt%. The Pt/Al<sub>2</sub>O<sub>3</sub> sample was cut into a 1-inch long core weighing about 3 g and having a cross-section of 60 channels. The total gas flow rate over this sample was 6.6 L min<sup>-1</sup> (space velocity of 80,500 h<sup>-1</sup>). The percentage of metal exposed (PME) or metal dispersion of this catalyst, defined as the ratio of the number of surface Pt atoms to the total number of Pt atoms, was measured by H<sub>2</sub>-O<sub>2</sub> titration [12] and was 42%. The Pt/BaO/Al<sub>2</sub>O<sub>3</sub> catalyst was cut into a 3-inch long core with a cross section of 60 cells. The total flow rate over this sample was 7.0 L min<sup>-1</sup> corresponding to a gas hourly space velocity of 30,000 h<sup>-1</sup>. The PME of Pt in this sample was 60%. This gives an exposed Pt content of 6.2 and 8.2 μmol g<sup>-1</sup> for the Pt/Al<sub>2</sub>O<sub>3</sub> and Pt/BaO/Al<sub>2</sub>O<sub>3</sub> samples, respectively.

The experimental apparatus used for this study is described in detail elsewhere [13] and briefly here. All the experiments reported here were run at 300 °C, except where specified. The

NO, NO<sub>2</sub>, N<sub>2</sub>O, NH<sub>3</sub> and H<sub>2</sub>O concentrations in the outlet gas stream were detected with an FTIR gas analyzer (MKS MultiGas™ Analyzer, Model 2030), while the N<sub>2</sub> concentration was detected with a quadrupole mass spectrometer (SRS RGA 200). The mass spectrometer was calibrated to measure N<sub>2</sub> concentrations in the 0–6500 ppm range either by the injection of pulses of known volumes of N<sub>2</sub> or by sampling calibrated N<sub>2</sub>/Ar mixtures. Argon was used as the carrier gas to allow for the measurement of the released N<sub>2</sub>. Mass flow controllers were used to control all the gas flows except for the experiments where high concentrations (>1000 ppm) of NH<sub>3</sub> and NO were utilized. These flows were controlled through needle valves. The system was automated to switch 3-way valves between lean-rich cycles. Thermocouples were placed 6 mm before and after the catalyst sample to verify inlet and outlet gas temperatures.

## 3. Results and discussion

Fig. 1 shows a comparison of the evolution of the outlet gas concentrations from a Pt/BaO/Al<sub>2</sub>O<sub>3</sub> catalyst after the switch to regeneration gases containing either H<sub>2</sub> or NH<sub>3</sub>. The solid lines indicate regeneration with 0.75% H<sub>2</sub>/Ar and the dashed lines indicate regeneration with 0.53% NH<sub>3</sub>/Ar. The number of hydrogen atoms per unit of time flowing over the sample in the regenerating gas mixture was kept nearly identical in both cases to illustrate the effectiveness of H<sub>2</sub> and NH<sub>3</sub> for regeneration. The regeneration phase (ca. 3 min long) was preceded by a 7 min long trapping (lean) phase that contained 350 ppm NO and 10% O<sub>2</sub>, balance Ar, and a 5 s purge with Ar. To obtain reproducible results, it was necessary to run 4–5 lean-rich cycles. The nitrogen balance between capture and regeneration phases was found to close within experimental error. After regeneration for 3 min with H<sub>2</sub> or NH<sub>3</sub>, the same amount of NO<sub>x</sub> was stored (0.54 mmol) during the subsequent 7-min capture phase, and the N<sub>2</sub> selectivities for both reductants were similar.

As seen in Fig. 1A, the N<sub>2</sub> and H<sub>2</sub>O traces for both regenerating mixtures increase rapidly to a constant value until the end when they sharply decrease. This rectangular wave shape indicates a “plug flow” type of mechanism implying a complete

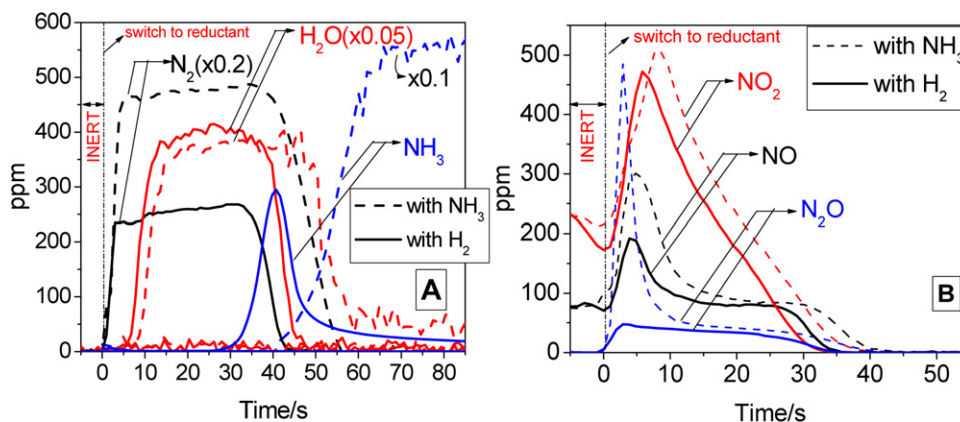


Fig. 1. Evolution of the species after the switch to the regeneration phase following a 7 min trapping period with 350 ppm NO/10%O<sub>2</sub>/Ar at 300 °C over a Pt/BaO/Al<sub>2</sub>O<sub>3</sub> monolith. The solid lines represent regeneration with 0.75% H<sub>2</sub>/Ar and the dashed lines represent regeneration with 0.53% NH<sub>3</sub>/Ar. The space velocity over the catalyst is 30,000 h<sup>-1</sup>. (A) N<sub>2</sub>, H<sub>2</sub>O and NH<sub>3</sub> traces, (B) NO<sub>2</sub>, NO and N<sub>2</sub>O traces.

reaction between the reductant and the NO<sub>x</sub> to produce N<sub>2</sub> and H<sub>2</sub>O. Since the reductant is the limiting reagent, this implies that the time for regeneration should be inversely proportional to the amount fed per unit time, as we verified experimentally. Note, however, that the data do not provide a mechanism for how the NO<sub>x</sub> is released from the trapping sites. Fig. 1A also shows that the H<sub>2</sub>O and N<sub>2</sub> traces in the case of NH<sub>3</sub> as the reductant continue at constant levels for a 15% longer duration before starting to decrease, when compared to the case with H<sub>2</sub> as the reductant. This difference is caused by the uncertainty in the reproducibility of the total flow rate. The H<sub>2</sub>O trace for NH<sub>3</sub> as a reductant did not return to zero because the NH<sub>3</sub>/Ar mixture contained H<sub>2</sub>O as an impurity. Accounting for this H<sub>2</sub>O impurity, the area under the H<sub>2</sub>O traces of Fig. 1A for the two reductants are the same within error (ca. 1.39 and 1.31 mmol). The N<sub>2</sub> level is higher when NH<sub>3</sub> is used as the reductant (0.74 mmol vs 0.22 mmol) since in addition to the nitrogen species in the stored NO<sub>x</sub>, NH<sub>3</sub> also contributes (through oxidation of NH<sub>3</sub> by the NO<sub>x</sub>) to the total N<sub>2</sub> formed. This makes the calculation of N<sub>2</sub> selectivity less precise.

Since the NH<sub>3</sub> and H<sub>2</sub> (H<sub>2</sub> data not shown since only non-quantifiably small H<sub>2</sub> amounts were observed in the mass spectrometer before breakthrough, and the H<sub>2</sub> concentration measurement was not precise) traces evolve close to the end of the cycle, the reductants are proposed to be limiting in the regeneration phase. As seen in Fig. 1A, NH<sub>3</sub> appears in the effluent (slips) only after 30–35 s into the regeneration cycle. The NH<sub>3</sub> (or H<sub>2</sub>) is consumed below detection level until this point and starts to slip only when the stored NO<sub>x</sub> starts to deplete toward the end of the catalyst bed. Thus, the shape of the NH<sub>3</sub> evolution curves for the H<sub>2</sub> and NH<sub>3</sub> cases are consistent with our plug flow model. In the case of regeneration by H<sub>2</sub>, the NH<sub>3</sub> evolution curve is the result of the competition between the generation (by NO<sub>x</sub>–H<sub>2</sub> reaction) and consumption (discussed below) of NH<sub>3</sub> at the end of the catalyst bed. In the case of regeneration by NH<sub>3</sub>, the NH<sub>3</sub> evolution curve has the characteristic “S” shape of strong gas adsorption seen, for example, during adsorption of NO<sub>2</sub> on BaO. Examining the NH<sub>3</sub> curves, we propose that the reason why NH<sub>3</sub> is seen only toward the end of the cycle must be due to the fact that the NH<sub>3</sub> front moves along the length of the catalyst bed in a plug flow manner while getting consumed in reducing NO<sub>x</sub> to N<sub>2</sub> (thereby regenerating the catalyst). When the NH<sub>3</sub> front reaches the end of the catalyst bed, it begins to break through due to the absence of NO<sub>x</sub> to oxidize the NH<sub>3</sub> to N<sub>2</sub> and H<sub>2</sub>O. This breakthrough is similar to the model presented by Epling et al. [14] for NO<sub>x</sub> storage, where the NO<sub>x</sub> sorption zone propagates down the catalyst bed in a plug flow manner and begins to breakthrough after reaching the end of the catalyst bed.

Experiments performed by varying the H<sub>2</sub> concentration in the regenerating phase over the range of 1.0–2.5% at the same total flow on the Pt/BaO/Al<sub>2</sub>O<sub>3</sub> catalyst (that has stored a similar NO<sub>x</sub> amount during the preceding capture phase) have shown that the time required for regeneration is inversely proportional to H<sub>2</sub> concentration. The selectivity to N<sub>2</sub> was maintained at 80–85%. In all cases, the evolution of H<sub>2</sub> (observed in the mass spectrometer) was delayed, indicating that the reduc-

tant was completely consumed during the initial stages of the regeneration phase. The time delay in evolution of H<sub>2</sub> decreased proportionally with increasing H<sub>2</sub> concentration as should be the case if the reductant is the limiting species in this reaction. We also observed that lowering the temperature for the tests to 242 °C made no difference on the reduction profiles, except that the amount of N<sub>2</sub>O produced was about twice as high. This insensitivity to temperature suggests that the regeneration is limited by transport of reactants and not by kinetics.

The sharp rise in the N<sub>2</sub> trace, as seen in Fig. 1A, implies that the H<sub>2</sub>O trace, the other product of the reduction reaction, should follow a similar profile. Although the curve shapes are similar, a delay is seen in the H<sub>2</sub>O trace, relative to N<sub>2</sub>, for both reductants. We investigated this phenomenon by including H<sub>2</sub>O (ca. 7.5%) in both the capture and regeneration phases. Interestingly, the usual NO<sub>x</sub> spike that arises immediately after the switch to the regeneration phase decreased by a factor of two compared to the dry feed conditions, and the H<sub>2</sub>O trace had a sharp rise similar to the N<sub>2</sub> trace (i.e., no delay) when H<sub>2</sub>O was included in the feed. In light of this data, we propose the following. It is well known that H<sub>2</sub>O decreases the NO<sub>x</sub> storage capacity of the NSR catalysts [4] and hence H<sub>2</sub>O could be competing for some of the NO<sub>x</sub> sites. In the absence of H<sub>2</sub>O in the trapping or lean-phase, the sites that generally favor the adsorption of H<sub>2</sub>O over NO<sub>x</sub> are occupied by NO<sub>x</sub>. However, when H<sub>2</sub>O is formed during the regeneration phase due to the reductant coming into contact with either residual O<sub>2</sub> or stored NO<sub>x</sub>, it first adsorbs on those sites that favor H<sub>2</sub>O adsorption over NO<sub>x</sub>, causing the delay in H<sub>2</sub>O evolution, while displacing the NO<sub>x</sub> that were stored on those sites, resulting in a larger NO<sub>x</sub> spike. When H<sub>2</sub>O is added to the feed during the trapping phase, it is preferentially adsorbed on some of the sites during the capture phase (decreasing NO<sub>x</sub> storage) and this prevents the adsorption of the H<sub>2</sub>O that is formed during the regeneration phase, resulting in the sharp rise (no delay) in the H<sub>2</sub>O trace and a decreased NO<sub>x</sub> spike. However, a small NO<sub>x</sub> spike (about 5% of total NO<sub>x</sub> stored) is still observed at the beginning of the regeneration phase even in the presence of H<sub>2</sub>O in the trapping phase. We hypothesize that this is due to the combination of desorption (explained below) and a few highly reactive sites that release NO<sub>x</sub> as a result of the low concentration of H<sub>2</sub> or NH<sub>3</sub> that contacts these sites in the initial phase of regeneration.

The NO and N<sub>2</sub>O traces in Fig. 1B are similar for both the reductants except for a higher initial spike with NH<sub>3</sub>. The concentration of NO and N<sub>2</sub>O (after the spike) is approximately constant with time. We propose that their shape is a result of depletion of H<sub>2</sub> at the end of the moving reduction front, and the reactions that take place in the non-reducing environment encountered there. In particular, we have observed that the reaction between NO and reduced Pt in the absence of adsorbed hydrogen will produce N<sub>2</sub>O until the surface is titrated to Pt–O and the reaction stops. Fig. 1B also shows that the NO<sub>2</sub> decrease (after the initial rise) is linear with time in both cases. We propose that this is simply due to the desorption of NO<sub>2</sub> arising from the shift in equilibrium between the surface and the gas phase that is accompanied with the switch to the re-

generating gases [9]. As the catalyst bed is reduced in a plug flow type mechanism, the amount of  $\text{NO}_2$  available for desorption ahead of the front decreases linearly with time, resulting in a linear decrease in  $\text{NO}_2$  evolution with time. To reinforce the hypothesis of  $\text{NO}_2$  desorption, we performed experiments with an inert substitute (Ar only with no reductant) in the regeneration phase spanning the same regeneration time period (ca. 3 min) as with  $\text{H}_2$ . After a 7 min trapping phase containing 350 ppm of NO, 10% of  $\text{O}_2$ , balance Ar, we observed 12% of the stored NOx desorbing as  $\text{NO}_2$  and 6% as NO under the inert flow conditions during the 3 min regeneration period compared to 7% as  $\text{NO}_2$ , 3% as NO under  $\text{H}_2$  rich conditions.

To summarize the findings,  $\text{NH}_3$  or  $\text{H}_2$  are capable of regenerating the trap in a similar way. We will investigate next the reaction of  $\text{NH}_3$  or  $\text{H}_2$  with NO over a Pt/ $\text{Al}_2\text{O}_3$  catalyst (without the trapping component) as a way to simulate the reduction steps (Figs. 2A and 2B). Most of the experiments were carried out under nearly isothermal conditions (300 °C). However, in experiments where a significant amount of  $\text{NH}_3$  was formed, the outlet gas temperature was 30–40 °C higher than that of the inlet. For this reason we carried out experiments at 200 °C to make sure the selectivity was not due to a hot spot. We observed similar product selectivity to that at 300 °C. The Pt/ $\text{Al}_2\text{O}_3$  monolith catalyst was first exposed to NO/Ar mixture for 2 min and then  $\text{H}_2$  (or  $\text{NH}_3$ ) was added to the NO flow at varying NO/reductant ratios for 6 min (the reactions reached steady state in less than 1 min). The data reported here was obtained by averaging the concentrations after 2 min of reaction. The NO/reductant ( $\text{H}_2$  or  $\text{NH}_3$ ) ratio was varied to simulate the different NOx/reductant environments that occur along the NSR trap.

As seen in Fig. 2 when all the reduction chemistry occurs on Pt, then the steady state selectivity to  $\text{N}_2$  is a strong function of the NO/reductant ratio. The  $\text{H}_2$  conversions noted in Fig. 2A were calculated based on the amounts of  $\text{N}_2$ ,  $\text{NH}_3$  and  $\text{N}_2\text{O}$  formed and the appropriate reaction stoichiometry, since the  $\text{H}_2$  concentration was not measured precisely. The selectivity to  $\text{N}_2$  is defined as the ratio of two times the total amount of  $\text{N}_2$  formed to the total amount of nitrogen species in the product ( $\text{NO}_2$ ,  $\text{N}_2\text{O}$ ,  $\text{NH}_3$ , and  $\text{N}_2$ ) formed during the reaction on

an atomic N basis. Fig. 2A shows that as the NO/ $\text{H}_2$  ratio increases from 0.4 (excess  $\text{H}_2$ ) to 4.6 (excess NO) the product selectivity changes from mostly  $\text{NH}_3$  at low NO/ $\text{H}_2$  ratios to  $\text{N}_2\text{O}$  at high NO/ $\text{H}_2$  ratios. The highest  $\text{N}_2$  selectivity was observed for a stoichiometric ratio (1:1) of NO/ $\text{H}_2$ . The formation of mostly  $\text{NH}_3$  under low NO/ $\text{H}_2$  ratios (reducing conditions) has previously been observed by Shelef et al. [15]. The product selectivities we have obtained for the NO/ $\text{H}_2$  reaction over the Pt/ $\text{Al}_2\text{O}_3$  sample are similar to that reported by Kosaki et al. [2] for their Pt/ $\text{Al}_2\text{O}_3$  powdered catalyst. Similarly, as the NO/ $\text{NH}_3$  ratio is varied from 0.67 (excess  $\text{NH}_3$ ) to 5 (excess NO), Fig. 2B, the product selectivity changes from mostly  $\text{N}_2$  at low NO/ $\text{NH}_3$  ratios to  $\text{N}_2\text{O}$  at high NO/ $\text{NH}_3$  ratios. Otto et al. [16] have previously shown that  $\text{NH}_3$  is an effective reductant in the removal of NO from waste effluents over supported Pt. Although similar experiments with  $\text{NO}_2 + \text{H}_2$  or  $\text{NH}_3$  were not performed, we expect similar results with respect to the product selectivity as with the experiments with NO described above, with the possibility of  $\text{NO}_2$  being more reactive. We have also carried out experiments involving  $\text{N}_2\text{O}$  and  $\text{H}_2$  at 300 °C over the Pt/ $\text{Al}_2\text{O}_3$  catalyst. In this case, with ca. 50 ppm  $\text{N}_2\text{O}$  and ca. 1%  $\text{H}_2$  at 300 °C, the  $\text{N}_2\text{O}$  was reduced to  $\text{N}_2$  and  $\text{H}_2\text{O}$  at a total conversion of 90%. These results for reduction with  $\text{H}_2$  or  $\text{NH}_3$  show that selectivity to  $\text{N}_2$  is high only in specific ranges of oxidant/reductant ratios. This information is important to the formulation of our regeneration model.

Fig. 3 shows a schematic of the proposed regeneration mechanism for a single monolith channel of a Pt/ $\text{BaO}/\text{Al}_2\text{O}_3$  NSR catalyst. The figure illustrates the propagation of the reductant front along the catalyst bed with complete regeneration of the trapping sites. A zoomed-in version of the chemistry occurring within the reductant front is also illustrated in Fig. 3. It shows that as the NOx ( $\text{NO} + \text{NO}_2$ ) is released from the trapping sites (the exact mechanism of release is not known), it reacts with  $\text{H}_2$  over Pt to form  $\text{NH}_3$ ,  $\text{N}_2$  and  $\text{N}_2\text{O}$  as the N-containing species. The selectivity of the individual species will depend on the local NOx/ $\text{H}_2$  concentration ratios as shown in Fig. 2A. In regions where the  $\text{H}_2$  level is high compared to the NOx, the reaction with the released NOx over Pt will form mostly  $\text{NH}_3$  and some  $\text{N}_2$ . The  $\text{NH}_3$  formed will further react with more NOx to

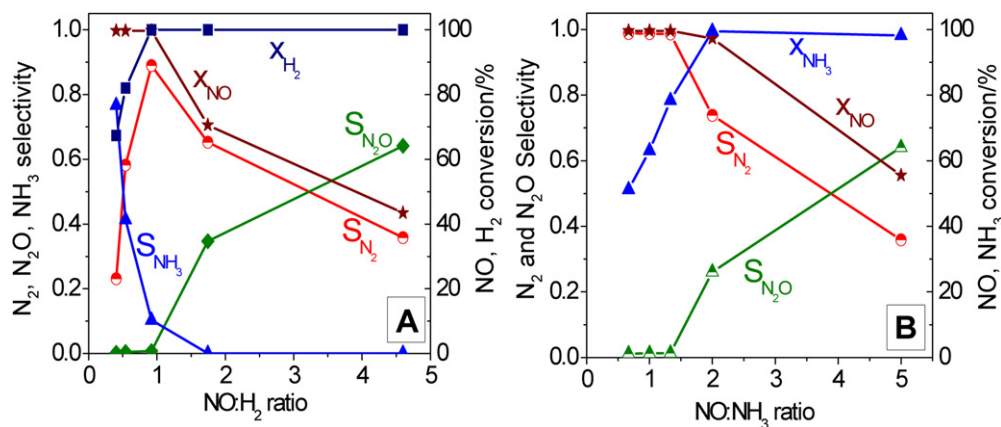


Fig. 2. Steady-state product selectivity and reactant conversion at 300 °C as a function of NO: reductant ratio for the reaction of (A)  $\text{NO} + \text{H}_2$  and (B)  $\text{NO} + \text{NH}_3$  over a Pt/ $\text{Al}_2\text{O}_3$  monolith.

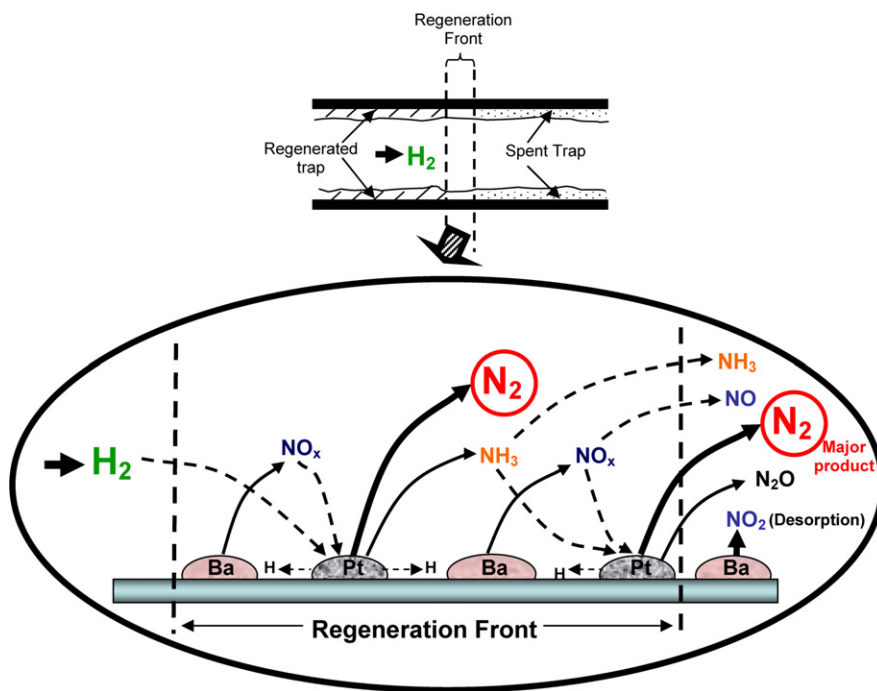


Fig. 3. Schematic of the reduction mechanism for a Pt/BaO/Al<sub>2</sub>O<sub>3</sub> monolith regenerated with H<sub>2</sub>. Bottom panel illustrates a zoomed-in picture of the reaction front.

give either N<sub>2</sub> or N<sub>2</sub>O. If the N<sub>2</sub>O is formed behind the front, it will be reduced to N<sub>2</sub> by H<sub>2</sub>/NH<sub>3</sub>. As the front approaches the end of the catalyst, the supply of NO<sub>x</sub> starts to deplete and will be insufficient to react with the NH<sub>3</sub> formed upstream, leading to the NH<sub>3</sub> breakthrough seen in Fig. 1A. Before the reaction front reaches the end of the bed, most of the non-selective products formed by the reaction of H<sub>2</sub> with NO<sub>x</sub> over Pt, such as N<sub>2</sub>O and NH<sub>3</sub>, will further react to form N<sub>2</sub> and maintain the high N<sub>2</sub> selectivity of the overall NSR catalyst. Using this rationale, and by reference to Fig. 2A, one might expect that as the concentration of H<sub>2</sub> is depleted at the end of the front, N<sub>2</sub>O should become a major product. This is not observed experimentally. We believe the reason is that there is a self-adjusting mechanism. As the concentration of H<sub>2</sub> is lowered, the amount of released NO is also lowered thus keeping the local overall ratio unfavorable to the formation of N<sub>2</sub>O. The N<sub>2</sub>O is formed in a stoichiometric reaction between Pt and NO to form N<sub>2</sub>O and Pt–O and is confined to the leading edge of the reaction front.

The reduction model proposed indicates that the trapping phase of the NSR cycle should not extend up to the full capacity of the trap since in that case the NO<sub>x</sub> released during regeneration would not be captured downstream. Furthermore, we propose that having an oxygen storage capacity (OSC) substrate such as ceria would allow the oxidation of NH<sub>3</sub> to N<sub>2</sub> when there are no more nitrates to oxidize it, and, hence, the OSC would decrease the NH<sub>3</sub> slip in the NSR catalysts.

#### 4. Conclusion

We have proposed a model for reduction by H<sub>2</sub> where NH<sub>3</sub> is the hydrogen carrier. In this model, derived from the results presented here, NO and NO<sub>2</sub> are first released into the gas phase and then reduced over Pt. It is not necessary to invoke a mech-

anism of surface diffusion of NO-containing species that are reduced on Pt. We propose a localized reaction front which travels through the bed with complete regeneration of the trapping sites as it propagates down the catalyst bed. This chemistry seems to be fast enough to make the process mass transfer limited and does not depend on whether the reactant is H<sub>2</sub> or NH<sub>3</sub>. Thus, the reaction kinetics and associated rate constants are not necessary to model the quantitative behavior of this system. The efficiency of the NSR catalyst in converting NO<sub>x</sub> to mostly N<sub>2</sub> is achieved because the other products that form over Pt, such as N<sub>2</sub>O and NH<sub>3</sub>, are either not favored (N<sub>2</sub>O) or can further react to produce N<sub>2</sub>. The low observed amounts of NO and N<sub>2</sub>O are explained by a self-limiting NO production rate as the H<sub>2</sub> concentration is depleted at the leading edge of the front. The hydrogen on the surface of Pt will react first to reduce NO and N<sub>2</sub>O before it will spillover to release more NO. As the hydrogen on the surface is depleted, the NO in the gas phase will adsorb and react on Pt to produce N<sub>2</sub>O until the surface is oxidized and the remaining NO will escape. The NO<sub>2</sub> profile is due to simple desorption. The NH<sub>3</sub> profile measured at the end of the cycle when using H<sub>2</sub> as a reductant is a result of insufficient NO<sub>x</sub> left in the bed to consume the NH<sub>3</sub> formed as the front reaches breakthrough.

#### Acknowledgments

The authors thank the Indiana 21st Century Research and Technology Fund and Cummins Inc. for financial support of this work.

#### References

- [1] M. Takeuchi, S.i. Matsumoto, *Top. Catal.* 28 (2004) 151.
- [2] Y. Kosaki, A. Miyamoto, Y. Murakami, *Chem. Lett.* 8 (1979) 935.

- [3] J. Siera, P. Cobden, K. Tanaka, B.E. Nieuwenhuys, *Catal. Lett.* 10 (1991) 335.
- [4] W.S. Epling, L.E. Campbell, A. Yezerets, N.W. Currier, J.E. Parks, *Catal. Rev.* 46 (2004) 163.
- [5] R. Burch, P.J. Millington, *Catal. Today* 26 (1995) 185.
- [6] T. Maunula, J. Ahola, H. Hamada, *Appl. Catal. B* 26 (2000) 173.
- [7] K.S. Kabin, R.L. Muncrief, M.P. Harold, *Catal. Today* 96 (2004) 79.
- [8] A. Amberntsson, H. Persson, P. Engstrom, B. Kasemo, *Appl. Catal. B* 31 (2001) 27.
- [9] Z. Liu, J.A. Anderson, *J. Catal.* 224 (2004) 18.
- [10] S. Poulston, R.R. Rajaram, *Catal. Today* 81 (2003) 603.
- [11] I. Nova, L. Lietti, L. Castoldi, E. Tronconi, P. Forzatti, *J. Catal.* 239 (2006) 244.
- [12] J.E. Benson, M. Boudart, *J. Catal.* 4 (1965) 704.
- [13] S.S. Mulla, N. Chen, L. Cumaratunge, W.N. Delgass, W.S. Epling, F.H. Ribeiro, *Catal. Today* 114 (2006) 57.
- [14] W.S. Epling, J.E. Parks, G.C. Campbell, A. Yezerets, N.W. Currier, L.E. Campbell, *Catal. Today* 96 (2004) 21.
- [15] M. Shelef, J.H. Jones, J.T. Kummer, K. Otto, E.E. Weaver, *Environ. Sci. Technol.* 5 (1971) 790.
- [16] K. Otto, M. Shelef, J.T. Kummer, *J. Phys. Chem.* 74 (1970) 2690.